

Crystal structure and solid-state fluorescence of an oxomolybdenum(V)–benzylviologen electron donor–acceptor salt

Abdul K. Mohammed, Frank R. Fronczek, Andrew W. Maverick *

Department of Chemistry, Louisiana State University, Baton Rouge, LA 70803-1804, USA

Received 15 April 1994

Abstract

Solutions containing benzylviologen and the fluorescent oxo- d^1 ion $\text{MoOBr}_4(\text{CH}_3\text{CN})^-$ in acetonitrile slowly deposit crystals of the electron donor–acceptor complex $(\text{BV})[\text{MoOBr}_4(\text{H}_2\text{O})]\text{Br} \cdot \text{CH}_3\text{CN}$: $\text{C}_{26}\text{H}_{27}\text{Br}_3\text{MoN}_3\text{O}_2$, triclinic, space group $P\bar{1}$; $a = 11.349(1)$, $b = 16.1048(8)$, $c = 18.720(1)$ Å; $\alpha = 71.961(5)$, $\beta = 76.375(7)$, $\gamma = 82.484(6)^\circ$; $Z = 4$; $R(F) = 0.048$, $R_w(F) = 0.046$ for 4135 reflections and 668 parameters. The two independent Mo complex anions in the structure show $\text{Mo}\equiv\text{O}$ distances of 1.62(1) and 1.629(9) Å. The fluorescence spectrum of the solid complex is similar in shape and intensity to those of other salts of $\text{Mo}^{\text{V}}\text{OBr}_4(\text{H}_2\text{O})^-$ with non-quenching cations. The relatively intense fluorescence of solid $(\text{BV})[\text{MoOBr}_4(\text{H}_2\text{O})]\text{Br} \cdot \text{CH}_3\text{CN}$ suggests that electron transfer from $\text{Mo}^{\text{V}}\text{OBr}_4(\text{H}_2\text{O})^-$ (^2E) to BV^{2+} , although slightly favorable thermodynamically, does not compete effectively with its rapid fluorescence.

Keywords: Crystal structures; Solid-state fluorescence; Molybdenum complexes; Oxo complexes; Benzylviologen salts

1. Introduction

Recently we began studying the photophysics and photoredox properties of Mo(V) oxo complexes [1,2]. These complexes, which have the d^1 electronic configuration, exhibit unusually long-lived fluorescences (25–110 ns) in solution at room temperature. In the course of our studies of the photoredox properties of $\text{MoOBr}_4(\text{CH}_3\text{CN})^-$, we explored its photochemical reactivity with the electron acceptor benzylviologen (BV^{2+}). We found that solutions prepared from $\text{MoOBr}_4(\text{CH}_3\text{CN})^-$ and BV^{2+} in acetonitrile slowly deposit yellow crystals. We have now identified the crystals as $(\text{BV})[\text{MoOBr}_4(\text{H}_2\text{O})]\text{Br} \cdot \text{CH}_3\text{CN}$ (**1**), an unusual example of a salt containing both an electron donor ($\text{Mo}^{\text{V}}\text{OBr}_4(\text{H}_2\text{O})^-$) and an electron acceptor (BV^{2+}). We report herein the crystal structure of **1** and its solid-state fluorescence, which is attributable to $\text{Mo}^{\text{V}}\text{OBr}_4(\text{H}_2\text{O})^-$. **1** fluoresces with approximately the same intensity as salts of $\text{Mo}^{\text{V}}\text{OBr}_4(\text{H}_2\text{O})^-$ with non-quenching cations. This indicates that electron

transfer from the fluorescent Mo^{V} excited state ($\text{Mo}^{\text{V}*}$) to BV^{2+} , though thermodynamically spontaneous ($\Delta G = -0.16$ eV), is significantly slower than fluorescence.

2. Experimental

2.1. Materials

Benzylviologen dichloride (Sigma Chemical Co.) was converted to the tetrafluoroborate salt by metathesis with NaBF_4 in methanol [3], and the resulting $\text{BV}(\text{BF}_4)_2$ was purified by recrystallization from aqueous ethanol. Other materials and solvents were reagent or spectrophotometric grade and were used as received.

$\text{Bu}_4\text{N}[\text{MoOBr}_4(\text{H}_2\text{O})]$ can be prepared by the method described by Bino and Cotton [4]. However, we also isolated the same complex by a different procedure. $\text{Et}_4\text{N}[\text{TpMo}(\text{CO})_3]$ [5] was refluxed in 9 M HBr for ~24 h, and the solution was allowed to cool to room temperature. Addition of excess Bu_4NBr in 9 M HBr to the cooled solution produced a deep orange–yellow crystalline precipitate of $\text{Bu}_4\text{N}[\text{MoOBr}_4(\text{H}_2\text{O})]$.

Yellow X-ray quality crystals of **1** formed in acetonitrile solutions containing $\text{Bu}_4\text{N}[\text{MoOBr}_4(\text{CH}_3\text{CN})]$

Abbreviations: BV^{2+} = benzylviologen (1,1'-dibenzyl-4,4'-bipyridinium); Tp^- = $\text{HB}(3,5\text{-Me}_2\text{pz})_3^-$ (hydrotris(3,5-dimethylpyrazol-1-yl)borate); $\text{TCNQ} = 7,7,8,8\text{-tetracyanoquinodimethane}$.

* Corresponding author.

(~ 0.05 M; prepared by dissolving $\text{Bu}_4\text{N}[\text{MoOBr}_4(\text{H}_2\text{O})]$ in CH_3CN) and $\text{BV}(\text{BF}_4)_2$ (~ 0.005 M) in CH_3CN on standing for 48–72 h at room temperature.

2.2. Spectroscopic measurements

IR spectra were recorded in compressed KBr pellets on a Perkin-Elmer model 1760X FT-IR spectrometer. Luminescence measurements were made on a Spex Industries Fluorolog 2 model F112X spectrometer (with Hamamatsu R406 PMT detector), and were corrected for the variation of detector sensitivity with wavelength. Solid samples for fluorescence measurements were ground in a mortar and placed in a 1 mm quartz spectrophotometer cell; enough material was used to fill the excitation beam completely. The samples were either pure **1** or a mixture of $\text{Bu}_4\text{N}[\text{MoOBr}_4(\text{H}_2\text{O})]$ diluted with enough KBr to provide the same percentage by mass of $\text{MoOBr}_4(\text{H}_2\text{O})^-$. Electronic absorption spectra were recorded on an Aviv 14DS spectrophotometer.

2.3. X-ray data collection, structure determination and refinement

A parallelepiped of $(\text{BV})[\text{Mo}^{\text{V}}\text{OBr}_4(\text{H}_2\text{O})]\text{Br} \cdot \text{CH}_3\text{CN}$ was mounted in a glass capillary in a random orientation (in the mother liquor from crystallization), and then placed on an Enraf-Nonius CAD4 computer controlled κ -axis diffractometer. Mo $K\alpha$ radiation was employed, with a graphite crystal monochromator in the incident beam. Cell constants were obtained from least-squares refinement using the setting angles of 25 reflections in the range $3 < \theta < 12^\circ$.

Crystallographic computations were performed on a MicroVAX II computer using the SDP/VAX crystal structure determination package [6]. The structure was solved by direct methods (MULTAN82) [7] and refined by full-matrix least-squares. The positions of the Mo and coordinated Br atoms were deduced from the initial E map. The remaining non-hydrogen atoms, including those of the CH_3CN solvent of crystallization, were located in successive difference Fourier maps. Positions of the hydrogen atoms in the BV^{2+} moieties were calculated. These hydrogen atoms were included in structure factor calculations but their positions and isotropic temperature factors were not refined; no other H atoms were included. The function minimized in refinement was $\sum w(|F_o| - |F_c|)^2$. Scattering factors and anomalous dispersion effects [8] were included in the calculation of F_c . A summary of data collection and refinement parameters is given in Table 1. Final atomic coordinates for non-hydrogen atoms are listed in Table 2. Interatomic bond distances and angles are collected in Tables 3 and 4, respectively. See also Section 5. An ORTEP [9] drawing of one of the two independent molecules in the asymmetric unit appears in Fig. 1.

Table 1
Data collection and refinement parameters for $(\text{BV})[\text{Mo}^{\text{V}}\text{OBr}_4(\text{H}_2\text{O})]\text{Br} \cdot \text{CH}_3\text{CN}^a$

Formula	$\text{C}_{26}\text{H}_{27}\text{Br}_5\text{MoN}_3\text{O}_2$
Formula weight	909.01
Color	yellow
Habit	parallelepiped
a (Å)	11.349(1)
b (Å)	16.1048(8)
c (Å)	18.720(1)
α (°)	71.961(5)
β (°)	76.375(7)
γ (°)	82.484(6)
V (Å ³)	3155.4(5)
Z	4
Space group	$P\bar{1}$
Temperature (°C)	28 ± 1
ρ_x (g cm ⁻³)	1.913
λ (Å)	0.71073 (Mo $K\alpha$)
μ (cm ⁻¹)	67.1
Crystal dimensions (mm)	$0.40 \times 0.42 \times 0.52$
Transmission coefficient	0.752–0.999
θ Range (°)	1–22.5
Scan type	ω -2 θ
Octants collected	$h \pm k \pm l$
Reflections measured	8232
Reflections observed ^b	4135
Parameters	668
Intensity standards	5.7% increase
$R(F)^c$	0.048
$R_w(F)^d$	0.046
GOF^e	1.707
Max. shift/e.s.d.	0.01
Max. residuals (e Å ⁻³)	0.74
Min. residuals (e Å ⁻³)	-0.22
Extinction ^f	$6.7(4) \times 10^{-8}$

^aIn Tables 1–4, e.s.d.s in the least significant digits of the values are given in parentheses.

^b $I > 3\sigma(I)$.

^c $R = \sum ||F_o| - |F_c|| / \sum |F_o|$.

^d $R_w = \sqrt{(\sum w(|F_o| - |F_c|)^2) / \sum w F_o^2}$; $w = 4F_o^2 / (\sigma^2(I) + (0.02F_o^2)^2)$.

^e $GOF = \sqrt{(\sum w(|F_o| - |F_c|)^2) / (N_{\text{obs}} - N_{\text{param}})}$.

^fCoefficient g in correction factor $(1 + gI_c)^{-1}$ applied to F_c .

3. Results and discussion

3.1. Electronic spectroscopy of metal-oxo complexes

A number of complexes with metal–ligand multiple bonds have been studied by spectroscopic and photochemical methods. Ballhausen and Gray analyzed the electronic absorption spectra of oxo-d¹ species, including the ‘vanadyl’ and ‘molybdenyl’ ions, in the early 1960s [10,11]. They proposed a simple bonding model (Fig. 2) which has been the basis for numerous subsequent studies. Early work by Rillema and Brubaker with Mo(V) and W(V) alkoxide complexes [12] showed that some of the Mo(V) oxo species can be generated photochemically. However, there was little direct study of their excited states until the mid-1980s, when the phosphorescences of $\text{ReO}_2(\text{py})_4^+$ and $\text{ReO}_2(\text{CN})_4^{3-}$ [13]

Table 2

Atomic coordinates for (BV)[Mo^VOBr₄(H₂O)]Br·CH₃CN

	x	y	z	U _{eq} (Å ²)
Mo1a	0.2220(1)	0.21063(8)	-0.00608(7)	0.0367(4)
Br1a	0.1638(2)	0.1462(1)	0.13741(8)	0.0606(6)
Br2a	0.0371(2)	0.3165(1)	-0.00264(9)	0.0601(6)
Br3a	0.2478(2)	0.2459(1)	-0.15050(9)	0.0598(6)
Br4a	0.3798(2)	0.0822(1)	-0.00779(9)	0.0679(6)
O1a	0.3187(8)	0.2769(6)	-0.0070(6)	0.060(4)
O2a	0.0914(8)	0.1143(5)	-0.0033(5)	0.049(3)
Br5a	0.0068(2)	0.93791(9)	0.12738(9)	0.0599(6)
N1a	0.4812(9)	0.8921(6)	0.2280(5)	0.035(4)
N2a	0.031(1)	0.5962(6)	0.3166(6)	0.041(4)
C1a	0.471(1)	0.8252(8)	0.2907(7)	0.047(5)
C2a	0.382(1)	0.7690(8)	0.3128(7)	0.047(5)
C3a	0.295(1)	0.7794(7)	0.2687(6)	0.031(4)
C4a	0.305(1)	0.8520(8)	0.2045(7)	0.041(5)
C5a	0.397(1)	0.9050(8)	0.1865(7)	0.042(5)
C6a	0.134(1)	0.5735(8)	0.3443(7)	0.041(5)
C7a	0.217(1)	0.6318(8)	0.3313(7)	0.039(5)
C8a	0.202(1)	0.7186(8)	0.2859(6)	0.033(4)
C9a	0.097(1)	0.7373(8)	0.2591(7)	0.044(5)
C10a	0.013(1)	0.6784(8)	0.2727(7)	0.040(5)
C11a	0.580(1)	0.9543(9)	0.2060(8)	0.056(6)
C12a	0.542(1)	1.0294(8)	0.2362(7)	0.042(5)
C13a	0.482(1)	1.103(1)	0.196(1)	0.087(7)
C14a	0.443(2)	1.171(1)	0.226(1)	0.15(1)
C15a	0.468(2)	1.168(1)	0.296(1)	0.174(9)
C16a	0.523(2)	1.097(1)	0.335(1)	0.127(8)
C17a	0.560(1)	1.0283(9)	0.3042(8)	0.067(6)
C18a	-0.060(1)	0.5289(9)	0.3318(8)	0.053(6)
C19a	-0.019(1)	0.4742(8)	0.2798(7)	0.044(5)
C20a	0.057(1)	0.3985(9)	0.2985(8)	0.056(6)
C21a	0.097(2)	0.3492(9)	0.2494(9)	0.074(7)
C22a	0.059(2)	0.3719(9)	0.1793(8)	0.076(6)
C23a	-0.017(1)	0.444(1)	0.1622(8)	0.076(6)
C24a	-0.052(1)	0.4938(9)	0.2118(8)	0.063(6)
N1sa	0.453(1)	0.3917(8)	0.0786(9)	0.112(7)
C1sa	0.379(2)	0.4297(9)	0.0419(9)	0.095(8)
C2sa	0.294(2)	0.476(1)	-0.0064(9)	0.090(7)
Mo1b	0.2919(1)	0.27310(8)	0.49933(7)	0.0397(4)
Br1b	0.1041(1)	0.3766(1)	0.51056(8)	0.0507(6)
Br2b	0.2296(2)	0.2043(1)	0.64314(9)	0.0671(7)
Br3b	0.4991(2)	0.1959(1)	0.50492(9)	0.0602(6)
Br4b	0.3697(2)	0.3701(1)	0.36527(9)	0.0635(6)
O1b	0.2344(8)	0.2032(6)	0.4722(5)	0.059(4)
O2b	0.3798(8)	0.3744(5)	0.5318(5)	0.050(3)
Br5b	0.3267(2)	0.58520(9)	0.50524(9)	0.0530(6)
N1b	0.248(1)	0.8031(7)	0.9438(6)	0.058(5)
N2b	0.128(1)	0.7813(7)	0.6002(6)	0.046(4)
C1b	0.294(1)	0.7350(9)	0.9161(7)	0.062(6)
C2b	0.279(1)	0.7333(8)	0.8478(8)	0.057(6)
C3b	0.214(1)	0.7982(8)	0.8035(7)	0.040(5)
C4b	0.169(1)	0.8688(9)	0.8310(7)	0.054(5)
C5b	0.184(1)	0.8704(9)	0.9020(8)	0.056(6)
C6b	0.221(1)	0.7333(8)	0.6265(7)	0.049(5)
C7b	0.251(1)	0.7394(8)	0.6916(7)	0.047(5)
C8b	0.187(1)	0.7949(8)	0.7322(7)	0.039(5)
C9b	0.090(1)	0.8439(9)	0.7023(7)	0.059(6)
C10b	0.063(1)	0.8368(9)	0.6376(8)	0.061(6)
C11b	0.258(2)	0.809(1)	1.0194(8)	0.079(7)
C12b	0.298(1)	0.7230(8)	1.0716(7)	0.043(5)
C13b	0.219(1)	0.657(1)	1.1052(7)	0.059(5)
C14b	0.260(2)	0.577(1)	1.1524(8)	0.071(6)

(continued)

Table 2 (continued)

	x	y	z	U _{eq} (Å ²)
C15b	0.373(1)	0.568(1)	1.1659(8)	0.072(7)
C16b	0.446(1)	0.635(1)	1.1332(9)	0.069(6)
C17b	0.409(1)	0.7120(9)	1.0876(8)	0.060(6)
C18b	0.100(1)	0.7720(9)	0.5303(8)	0.056(6)
C19b	0.124(1)	0.8536(8)	0.4631(7)	0.048(5)
C20b	0.207(1)	0.912(1)	0.4554(9)	0.065(6)
C21b	0.231(2)	0.982(1)	0.389(1)	0.088(8)
C22b	0.168(2)	0.989(1)	0.3318(8)	0.089(7)
C23b	0.083(2)	0.934(1)	0.3373(9)	0.083(7)
C24b	0.063(2)	0.868(1)	0.4036(9)	0.071(6)
N1sb	0.344(1)	0.5380(9)	0.7805(8)	0.094(6)
C1sb	0.379(1)	0.495(1)	0.736(1)	0.095(7)
C2sb	0.420(2)	0.441(1)	0.6883(8)	0.080(7)

$$^*U_{eq} = 1/3(a^2a^{*2}U_{11} + b^2b^{*2}U_{22} + c^2c^{*2}U_{33} + 2aba^*b^*U_{12} \cos \gamma + 2aca^*c^*U_{13} \cos \beta + 2bcb^*c^*U_{23} \cos \alpha).$$

Table 3

Interatomic distances (Å) for (BV)[Mo^VOBr₄(H₂O)]Br·CH₃CN^a

	a	b	a	b	
Mo1-Br1	2.519(2)	2.538(2)	C8-C9	1.36(2)	1.39(2)
Mo1-Br2	2.526(2)	2.537(2)	C9-C10	1.36(2)	1.36(2)
Mo1-Br3	2.537(2)	2.521(2)	C11-C12	1.46(2)	1.51(2)
Mo1-Br4	2.556(2)	2.531(2)	C12-C13	1.38(2)	1.38(2)
Mo1-O1	1.62(1)	1.629(9)	C12-C17	1.33(2)	1.34(2)
Mo1-O2	2.263(9)	2.314(9)	C13-C14	1.37(3)	1.41(2)
N1-C1	1.32(2)	1.35(2)	C14-C15	1.39(5)	1.35(2)
N1-C5	1.33(2)	1.36(2)	C15-C16	1.31(5)	1.35(2)
N1-C11	1.50(2)	1.48(2)	C16-C17	1.38(3)	1.35(2)
N2-C6	1.36(2)	1.32(2)	C18-C19	1.47(2)	1.51(2)
N2-C10	1.34(2)	1.34(2)	C19-C20	1.40(2)	1.37(2)
N2-C18	1.51(2)	1.47(2)	C19-C24	1.34(2)	1.39(2)
C1-C2	1.35(2)	1.34(2)	C20-C21	1.36(2)	1.40(2)
C2-C3	1.39(2)	1.37(2)	C21-C22	1.41(2)	1.39(3)
C3-C4	1.39(2)	1.38(2)	C22-C23	1.35(2)	1.36(3)
C3-C8	1.44(2)	1.46(2)	C23-C24	1.37(2)	1.35(2)
C4-C5	1.35(2)	1.39(2)	N1s-C1s	1.19(3)	1.21(3)
C6-C7	1.35(2)	1.38(2)	C1s-C2s	1.46(3)	1.39(3)
C7-C8	1.41(2)	1.38(2)			

^aIn Tables 3 and 4, the headings 'a' and 'b' denote data for atoms labeled 'a' and 'b' in Table 2.

and of a tungsten carbyne complex [14] were first reported. Since then, a variety of metal-ligand multiply bonded systems, including d² species containing the ReO₂⁺ and ReN²⁺ chromophores, have been found to luminesce and to undergo photochemical redox reactions.

In the oxo-d² species, the ground state is ¹A₁ (see Fig. 2; C_{4v} symmetry assumed), arising from the (b₂)² configuration, and the emission is phosphorescence (³E → ¹A₁, e → b₂). Luminescence from oxo-d¹ complexes was first observed by Winkler [15] in crystals containing the square-pyramidal MoOX₄⁻ ions (X = halogen). In these complexes, there are no spin-forbidden d-d transitions, and the luminescence is one of the few examples of fluorescence (²E → ²B₂, e → b₂) in a transition-metal

Table 4
Bond angles (°) for (BV)[Mo^VOBr₄(H₂O)]Br·CH₃CN

	a	b	a	b
Br1–Mo1–Br2	90.12(8)	87.23(7)	N1–C5–C4	123(1)
Br1–Mo1–Br3	165.49(9)	164.49(9)	N2–C6–C7	122(1)
Br1–Mo1–Br4	87.84(7)	89.48(7)	C6–C7–C8	121(1)
Br1–Mo1–O1	97.4(4)	97.4(4)	C3–C8–C7	121(1)
Br1–Mo1–O2	81.8(2)	83.7(2)	C3–C8–C9	125(1)
Br2–Mo1–Br3	89.89(7)	88.45(7)	C7–C8–C9	114(1)
Br2–Mo1–Br4	168.83(9)	166.43(9)	C8–C9–C10	125(1)
Br2–Mo1–O1	96.9(3)	97.7(4)	N2–C10–C9	119(1)
Br2–Mo1–O2	84.9(3)	85.0(3)	N1–C11–C12	112(1)
Br3–Mo1–Br4	89.35(7)	91.26(8)	C11–C12–C13	121(2)
Br3–Mo1–O1	97.0(4)	97.9(4)	C1–C12–C17	122(2)
Br3–Mo1–O2	83.7(2)	81.1(2)	C13–C12–C17	118(2)
Br4–Mo1–O1	94.2(3)	95.8(4)	C12–C13–C14	121(2)
Br4–Mo1–O2	84.0(3)	81.6(3)	C13–C14–C15	119(3)
O1–Mo1–O2	178.1(4)	177.1(5)	C14–C15–C16	120(3)
C1–N1–C5	117(1)	120(1)	C15–C16–C17	120(3)
C1–N1–C11	122(1)	124(1)	C12–C17–C16	123(2)
C5–N1–C11	121(1)	116(1)	N2–C18–C19	110(1)
C6–N2–C10	119(1)	119(1)	C18–C19–C20	121(2)
C6–N2–C18	120(1)	118(1)	C18–C19–C24	122(2)
C10–N2–C18	121(1)	122(1)	C20–C19–C24	116(2)
N1–C1–C2	123(1)	121(1)	C19–C20–C21	122(2)
C1–C2–C3	120(1)	123(1)	C20–C21–C22	120(2)
C2–C3–C4	115(1)	117(1)	C21–C22–C23	118(2)
C2–C3–C8	123(1)	124(2)	C22–C23–C24	120(2)
C4–C3–C8	121(1)	119(1)	C19–C24–C23	124(2)
C3–C4–C5	121(1)	121(1)	N1s–C1s–C2s	177(3)

complex. More recently, we showed that a variety of Mo^V oxo complexes MoOX₄L[−] (L = neutral ligand) also fluoresce in solution at room temperature, with lifetimes as long as 100 ns, and that they can be photooxidized by electron acceptors [1].

3.2. Preparation, crystallization and fluorescence of (BV)[MoOBr₄(H₂O)]Br·CH₃CN

We previously showed [1] that the powerful electron acceptor tetracyanoethylene (TCNE; $E_{1/2} = -0.16$ V versus Fc⁺/Fc [16]) quenches the fluorescent excited state of MoOBr₄(CH₃CN)[−] ($E_{1/2}(\text{Mo}^{\text{VI}/\text{V}*}) = -0.92$ V versus Fc⁺/Fc) efficiently in CH₃CN solution at room temperature. This is illustrated in reaction (1) below. We were also interested in comparing the rates of quenching and back-electron transfer steps with neutral and cationic acceptors. One of the most promising cationic acceptors appeared to be benzylviologen (BV²⁺; $E_{1/2} = -0.76$ V versus Fc⁺/Fc in CH₃CN), which is among the easiest to reduce of the viologen family of pyridinium ions [17]. Quenching with BV²⁺ should occur according to reaction (2).

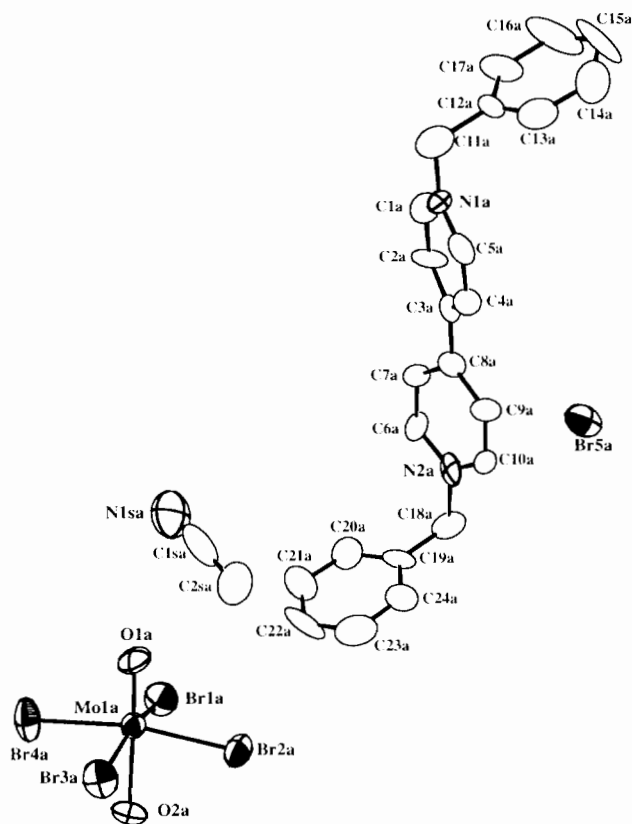
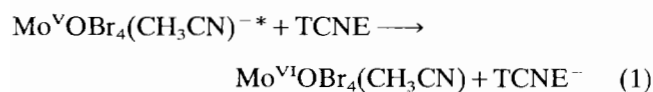


Fig. 1. ORTEP [9] diagram of (BV)[Mo^VOBr₄(H₂O)]Br·CH₃CN, with ellipsoids at the 50% probability level. Molecule 'a' is shown; the geometry of molecule 'b' is similar.

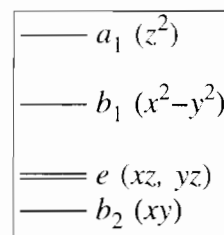
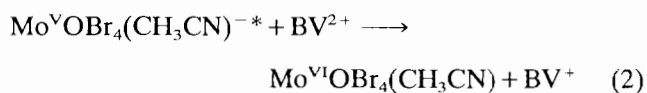


Fig. 2. Molecular orbital diagram for metal-oxo complexes MOX₄L (C_{4v} symmetry), after Refs. [10] and [11].



Although BV²⁺ is a poorer electron acceptor than TCNE, we anticipated that the opposite charges of chromophore and quencher in reaction (2) might still lead to efficient quenching. Also, the BV⁺ radical cation is deeply colored, with ϵ_{max} (603 nm) $\sim 1.5 \times 10^4 \text{ M}^{-1} \text{ cm}^{-1}$ [18], which should make it easy to detect by flash kinetic spectroscopy. However, neither a loss of fluorescence intensity nor transient signals characteristic of BV⁺ was observed when the experiments were performed.

In the course of these experiments, yellow crystals formed in CH₃CN solutions containing MoOBr₄-

(CH₃CN)⁻ and BV²⁺; we have now identified them as **1**. (Although the crystals are yellow, they appear slightly bluish, by comparison, when immersed in the mother liquor. This bluish color is probably due to the high-energy ‘tail’ of the ²B₂ → ²E transition centered at 720 nm [1], which is shifted slightly to higher energy in the H₂O complex relative to the CH₃CN solution, and is also considerably more intense in the concentrated crystals than in the solution).

Compound **1** contains both an electron acceptor (BV²⁺) and donor (MoOBr₄(H₂O)⁻). Similar donor–acceptor salts often exhibit low-energy bands in their electronic spectra that are attributable to charge-transfer transitions [19,20]. However, we found no such bands in the absorption spectra, either for solid **1** (KBr pellet) or for solutions containing BV²⁺ and MoOBr₄(H₂O)⁻.

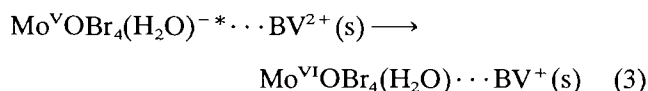
In our previous work [1] we showed that the fluorescent excited states Mo^VO* (²E) undergo oxidative quenching by several acceptors. (See the discussion of reactions (1) and (2) above.) We were somewhat surprised to find that benzylviologen did not quench the fluorescence of these ions measurably, because reaction of an excited molecule with a quencher of opposite charge is often strongly favored on electrostatic grounds. The new donor–acceptor salt **1** gave us an unusual opportunity to check if luminescence of MoOBr₄(H₂O)⁻ would be quenched by BV²⁺ in the solid state. However, solid **1** still fluoresces (see Fig. 3) with approximately the same intensity as solid Bu₄N[MoOBr₄(H₂O)].

3.3. Electron-transfer rates

As mentioned above, the fluorescences of Mo^V in CH₃CN solution are not quenched significantly in the presence of BV²⁺. There are several possible causes for this lack of quenching. First, the maximum concentration of BV²⁺ available in these experiments is

relatively low (~0.01 M). Second, the excited-state lifetimes of the Mo^V complexes are short (25–110 ns) [1]. Finally, since Δ*G* for reaction (2) is not highly negative (−0.16 eV), *k*₂ is expected to be well below the diffusion limit [21]. All of these factors combine to make it unlikely that oxidative quenching of Mo^VOBr₄(H₂O)^{-*} by BV²⁺ can compete effectively with the decay of the Mo^V excited state.

On the other hand, the *solid-state* fluorescence of **1** is more informative, because the quenching reaction in the solid state is now first-order, as shown in reaction (3).



1 and (Bu₄N)[Mo^VOBr₄(H₂O)] fluoresce with approximately the same intensity. This suggests that the solid-state quenching rate constant *k*₃ is smaller than the ²E → ²B₂ fluorescence decay rate for Mo^VOBr₄(H₂O)⁻, which is ~4 × 10⁷ s⁻¹ (assuming that the photophysics of Mo^VOBr₄(H₂O)⁻ is similar in CH₂Cl₂ solution [1] and in solid **1**). Thus, even in the solid state, where there are close contacts between Mo(V) and viologen ions (shortest anion–cation distances O2a ··· C5b, 3.28(2) Å, Br1b ··· N2a, 3.37(1) Å; shortest Mo–cation distances Mo1a ··· C5b, 4.75(1) Å, Mo1b ··· N2a, 5.12(1) Å) electron-transfer quenching is not fast enough to compete effectively with fluorescence decay.

Our failure to observe quenching of Mo^VOBr₄(H₂O)^{-*} in solid **1** could indicate that our estimates of electrode potentials in solution are not valid in the solid state. However, the above upper limit for *k*₃ is consistent with recent studies of intramolecular electron transfer rates. For example, Fox et al. recently examined binuclear iridium(I) complexes with coordinated electron acceptor groups [22]. For reactions of Δ*G* = −0.08 and −0.21 eV, they found rate constants of 3.5 × 10⁶ and 1.7 × 10⁸ s⁻¹ respectively. Thus, the lack of quenching in solid **1** is consistent with the potentials we have observed in solution.

Experiments with other electron acceptors, especially more powerful ones, would have enabled us to carry out a more systematic analysis of the electron-transfer properties of these Mo^V oxo complexes. However, very few other acceptors are available that are as powerful as BV²⁺ and TCNE.

3.4. Description of the structure of (BV)[MoOBr₄(H₂O)]Br · CH₃CN

The compound crystallizes in the triclinic space group *P*1̄ (No. 2), with two benzylviologen (BV²⁺) cations, two Mo^VOBr₄(H₂O)⁻ complex anions, two bromide anions and two molecules of CH₃CN in the asymmetric

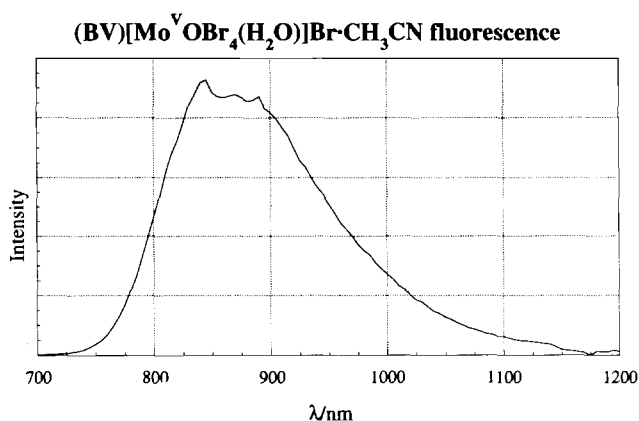


Fig. 3. Solid-state fluorescence spectrum of (BV)[Mo^VOBr₄(H₂O)]Br · CH₃CN at room temperature, corrected for detector response. Excitation wavelength 436 nm; emission bandpass 30 nm.

unit. The atoms of the two crystallographically independent formula units have been labeled 'a' and 'b' in Tables 2–4. Fig. 1 shows an ORTEP drawing of the 'a' formula unit. There is no obvious symmetry relationship between molecules 'a' and 'b'.

The crystal structures of the pyridinium, tetraethylammonium, and tetraphenylarsonium salts of the $\text{Mo}^{\text{V}}\text{OBr}_4(\text{H}_2\text{O})^-$ anion have been reported previously [4,23]. The Mo anions in **1** have similar pseudo-octahedral structures: the four equatorial Br^- ligands in molecules a and b are planar within 0.036 and 0.020 Å, respectively, and the Mo atoms are displaced out of that plane, toward the oxo group, by 0.282(1) (molecule a) and 0.317(1) (molecule b) Å.

The bond lengths in the two anion complexes a and b are quite similar. Our distances (see Table 3) are also very close to the following values found by Bino and Cotton [4]: $\text{Mo}\equiv\text{O}$, 1.62(2) Å; $\text{Mo}-\text{Br}$, 2.53(1) Å (av.); $\text{Mo}-\text{OH}_2$, 2.32(2) Å. Terminal $\text{Mo}\equiv\text{O}$ bond lengths for monooxo Mo complexes are normally in the range 1.65–1.70 Å [24]. $\text{M}\equiv\text{O}$ bond distances are often longer in six-coordinate *trans*- MOX_4L complexes than in the five-coordinate MoOX_4^- analogs; for example, the $\text{Mo}\equiv\text{O}$ bond lengths for $\text{Ph}_4\text{As}[\text{MoOCl}_4]$ and $\text{Ph}_4\text{As}[\text{MoOCl}_4(\text{H}_2\text{O})]$ are 1.61(1) [25] and 1.67(2) [26] Å, respectively. However, both in this work and in the previous study of Bino and Cotton, the $\text{Mo}\equiv\text{O}$ distances are relatively short, both similar to that found for $\text{Ph}_4\text{As}[\text{MoOCl}_4]$. The reason for this is unclear.

There is evidence for hydrogen bonding between the H atoms of the H_2O ligands and the Br^- counterions in the structure of **1**. Each Br^- is close to one H atom in each of two different $\text{MoOBr}_4(\text{H}_2\text{O})^-$ complexes, in a chain-like arrangement. The $\text{O}\cdots\text{Br}$ distances (see Table 3) are within the range expected (3.17–3.38 Å) for hydrogen bonds [27]; also, small peaks were observed (in positions that are reasonable for H atoms) between the O and Br atoms in the final difference Fourier calculations. We believe this hydrogen bonding contributes substantially to the stability of the crystal structure **1**. This interaction, which cannot occur in salts of the starting material $\text{MoOBr}_4(\text{CH}_3\text{CN})^-$, may be responsible for the preferential crystallization of compound **1** even in the presence of a large excess of CH_3CN .

Each benzylviologen cation in the present structure consists of a bipyridinium group and two benzyl groups. A search of the Cambridge Crystallographic Database [28] revealed two other X-ray analyses of benzylviologen salts: $(\text{BV})\text{I}_2$ [29] and $(\text{BV})(\text{TCNQ})_4$ [30]. The bond distances and angles within the BV^{2+} cations in **1** are similar to those in the two previously published structures. Also, the dihedral angles between the phenyl

rings and the nearest pyridine rings in **1** (112(1) and 110(1)° in molecule a; 114(1) and 112(1)° in molecule b) are similar to those in $(\text{BV})\text{I}_2$ (108°) and $(\text{BV})(\text{TCNQ})_4$ (113°). The most readily apparent difference is in the geometry of the bipyridinium moieties. The pyridine rings in the present structure are twisted relative to each other, with dihedral angles of 22.7(9) and 20(1)° for molecules a and b, respectively. In contrast, in both of the previous BV^{2+} structures, the cations lie on centers of symmetry; thus, the two rings of their bipyridinium moieties are constrained to be parallel.

4. Conclusions

The reaction of a benzylviologen salt $(\text{BV}(\text{BF}_4)_2)$ with the Mo^{V} oxo complex $(\text{Mo}^{\text{V}}\text{OBr}_4(\text{CH}_3\text{CN})^-)$ and H_2O in CH_3CN at room temperature leads to displacement of coordinated CH_3CN and crystallization of $(\text{BV})[\text{Mo}^{\text{V}}\text{OBr}_4(\text{H}_2\text{O})]\text{Br}\cdot\text{CH}_3\text{CN}$ (**1**). X-ray analysis of **1** shows that the geometry of its component ions is similar to that previously reported for $\text{Mo}^{\text{V}}\text{OBr}_4(\text{H}_2\text{O})^-$ and BV^{2+} . The d–d fluorescence of $\text{Mo}^{\text{V}}\text{OBr}_4(\text{H}_2\text{O})^-$ in **1** is not significantly quenched by BV^{2+} ions even in the solid state. This is due to a combination of the relatively short lifetime of $\text{Mo}^{\text{V}}\text{OBr}_4(\text{H}_2\text{O})^-$ (~25 ns in CH_2Cl_2 at room temperature) and the small driving force for the excited-state electron transfer ($\Delta G = -0.16$ eV).

Among the areas of interest for these complexes is altering the thermodynamics of their redox reactions, so that they can be studied using a wider variety of electron-transfer quenchers. This will be of use both for a comparison of rates and thermodynamics (as discussed above) and to provide a better match with the requirements of useful redox reactions. We also plan to compare our results with those recently reported for d^2 oxo [31,32] and nitrido [33] complexes.

5. Supplementary material

Tables of calculated hydrogen-atom coordinates, anisotropic displacement parameters, and observed and calculated structure factors are available from the authors.

Acknowledgements

This research was supported by grants from the National Science Foundation (CHE-8601008) and the Louisiana Educational Quality Support Fund (LEOSF(1990-92)-RD-A-06) administered by the Louisiana Board of Regents.

¹ The geometry of $\text{MoOCl}_4(\text{H}_2\text{O})^-$ in $(\text{Et}_4\text{N})_3(\text{H}_5\text{O}_2)[\text{Mo}_2\text{Cl}_8\text{H}][\text{MoOCl}_4(\text{H}_2\text{O})]$ [26] is similar.

References

- [1] A.K. Mohammed and A.W. Maverick, *Inorg. Chem.*, **31** (1992) 4441.
- [2] A.W. Maverick, Q. Yao, A.K. Mohammed and L.J. Henderson, Jr., *Adv. Chem. Ser.*, **238** (1993) 131.
- [3] S. Hunig, J. Groß, E.F. Lier and H. Quast, *Justus Liebigs Ann. Chem.*, (1973) 339.
- [4] A. Bino and F.A. Cotton, *Inorg. Chem.*, **18** (1979) 2710.
- [5] S. Trofimenko, *J. Am. Chem. Soc.*, **89** (1967) 6288; **91** (1969) 588.
- [6] B.A. Frenz, *SDP/VAX: Structure Determination Package*, B.A. Frenz and Associates, Inc., College Station, TX, USA and Enraf-Nonius, Delft, Netherlands, 1982.
- [7] P. Main, J.S. Fiske, S.E. Hull, L. Lessinger, G. Germain, J.-P. Declercq and M.M. Woolfson, *MULTAN82*, A system of computer programs for the automatic solution of crystal structures from X-ray diffraction data, Universities of York, UK and Louvain, Belgium, 1982.
- [8] D.T. Cromer and J.T. Waber, *International Tables of X-ray Crystallography*, Vol. IV, Kynoch, Birmingham, UK, 1974, pp. 71–147; 148–151.
- [9] C.K. Johnson, *ORTEP-II*, a Fortran thermal-ellipsoid plot program for crystal structure illustrations, *Rep. ORNL-5138*, Oak Ridge National Laboratory, National Technical Information Service, US Department of Commerce, Springfield, VA, USA, 1976.
- [10] C.J. Ballhausen and H.B. Gray, *Inorg. Chem.*, **1** (1962) 111.
- [11] H.B. Gray and C.R. Hare, *Inorg. Chem.*, **1** (1962) 363.
- [12] D.P. Rillema and G.R. Brubaker, *Inorg. Chem.*, **8** (1969) 1645; D.P. Rillema, W.J. Reagan and G.R. Brubaker, *Inorg. Chem.*, **8** (1969) 587.
- [13] J.R. Winkler and H.B. Gray, *J. Am. Chem. Soc.*, **105** (1983) 1373; *Inorg. Chem.*, **24** (1985) 346.
- [14] A.B. Bocarsly, R.E. Cameron, H.-D. Rubin, G.A. McDermott and A. Mayr, *Inorg. Chem.*, **24** (1985) 3976.
- [15] J.R. Winkler, *Ph.D. Thesis*, California Institute of Technology, Pasadena, CA, USA, 1984.
- [16] Q. Yao and A.W. Maverick, *J. Am. Chem. Soc.*, **108** (1986) 5364.
- [17] C.L. Bird and A.T. Kuhn, *Chem. Soc. Rev.*, **10** (1981) 49.
- [18] K. Tsukahara and R.G. Wilkins, *J. Am. Chem. Soc.*, **107** (1985) 2632.
- [19] A.J. MacFarlane and R.J.P. Williams, *J. Chem. Soc. A*, (1969) 1517.
- [20] C.K. Prout and P. Murray-Rust, *J. Chem. Soc. A*, (1969) 1520.
- [21] R.A. Marcus and N. Sutin, *Biochim. Biophys. Acta*, **811** (1985) 265.
- [22] L.S. Fox, M. Kozik, J.R. Winkler and H.B. Gray, *Science*, **247** (1990) 1069.
- [23] J.G. Scane, *Acta Crystallogr.*, **23** (1967) 85.
- [24] W.A. Nugent and J.M. Mayer, *Metal-Ligand Multiple Bonds*, Wiley, New York, 1988, p. 164.
- [25] C.D. Garner, L.H. Hill, F.E. Mabbs, D.L. McFadden and A.T. McPhail, *J. Chem. Soc., Dalton Trans.*, (1977) 853.
- [26] C.D. Garner, L.H. Hill, F.E. Mabbs, D.L. McFadden and A.T. McPhail, *J. Chem. Soc., Dalton Trans.*, (1977) 1202; A. Bino and F.A. Cotton, *J. Am. Chem. Soc.*, **101** (1979) 4150.
- [27] G.H. Stout and L.H. Jensen, *X-ray Structure Determination: A Practical Guide*. Macmillan, New York, 1968, p. 303.
- [28] F.H. Allen, O. Kennard and R. Taylor, *Acc. Chem. Res.*, **16** (1983) 146.
- [29] J.H. Russell and S.C. Wallwork, *Acta Crystallogr., Sect. B*, **27** (1971) 2473.
- [30] T. Sundaresan and S.C. Wallwork, *Acta Crystallogr., Sect. B*, **28** (1972) 2474.
- [31] H.H. Thorp, J. Van Houten and H.B. Gray, *Inorg. Chem.*, **28** (1989) 889.
- [32] W. Liu, T.W. Welch and H.H. Thorp, *Inorg. Chem.*, **31** (1992) 4044.
- [33] W.J. Vining, G.A. Neyhart, S. Nielsen and B.P. Sullivan, *Inorg. Chem.*, **32** (1993) 4214, and refs. therein.